



**HAL**  
open science

## Impacts of lithological and anthropogenic factors affecting water chemistry in the Upper Paraguay River Basin

Ary T Rezende-Filho, Vincent Vallès, Sonia Furian, Célia M.S.C. Oliveira, Jamila Ouardi, Laurent Barbiero

► **To cite this version:**

Ary T Rezende-Filho, Vincent Vallès, Sonia Furian, Célia M.S.C. Oliveira, Jamila Ouardi, et al.. Impacts of lithological and anthropogenic factors affecting water chemistry in the Upper Paraguay River Basin. *Journal of Environmental Quality*, 2015, 44 (6), pp.1832. hal-02043214

**HAL Id: hal-02043214**

**<https://hal.science/hal-02043214>**

Submitted on 20 Feb 2019

**HAL** is a multi-disciplinary open access archive for the deposit and dissemination of scientific research documents, whether they are published or not. The documents may come from teaching and research institutions in France or abroad, or from public or private research centers.

L'archive ouverte pluridisciplinaire **HAL**, est destinée au dépôt et à la diffusion de documents scientifiques de niveau recherche, publiés ou non, émanant des établissements d'enseignement et de recherche français ou étrangers, des laboratoires publics ou privés.

## **Impacts of lithological and anthropogenic factors affecting water chemistry in the Upper Paraguay River Basin**

**Ary T. Rezende-Filho<sup>1</sup>, Vincent Valles<sup>2</sup>, Sônia Furian<sup>3</sup>, Célia M.S.C. Oliveira<sup>4</sup>, Jamila Ouardi<sup>5</sup>, Laurent Barbiero<sup>6,7\*</sup>**

1 – Federal University of South Mato Grosso (UFMS), Geography Department, Cidade Universitária s/n, C.P. 549, 79070-900 Campo Grande-MS, Brazil

2 – University of Avignon et des Pays du Vaucluse, Applied Hydrogeology Laboratory, 74 Rue Louis Pasteur, F-84029 Avignon Cedex 01, France

3 – University of Sao Paulo, Geography Department, C.P. 8105, 05508-900, Sao Paulo, Brazil

4 – Federal University of South Mato Grosso (UFMS), Chemistry Department, Cidade Universitária, Av. Senador Filinto Müller 1555, 79074-460, Campo Grande-MS, Brazil

5 – Regional Centre for Careers in Education and Training (CRMEF), B.P. 294, Eljadida, Morocco

6 – University Paul Sabatier, Research Institute for the Development, National Centre of Scientific Research, Midi-Pyrénées Observatory, GET laboratory, 14 Av. E. Belin, F-31400 Toulouse, France

7 – University of Sao Paulo, Center for Nuclear Energy in Agriculture, Av. Centenário 303, CEP 13400-970, Piracicaba - São Paulo, Brazil

\* laurent.barbiero@get.obs-mip.fr

## **Impacts of lithological and anthropogenic factors affecting water chemistry in the Upper Paraguay River Basin**

**Abstract:** Located in the Upper Paraguay River Basin (UPRB), the Pantanal is considered the world's largest wetland, being rather pristine although increasingly threatened by development programs. The main objective of this paper is to provide a baseline of water chemistry for this region, which is largely unknown due to poor accessibility. We used two datasets (70 and 122 water samples) collected in the Pantanal floodplain and surrounding uplands during the wet season occurring from November to March. From the major ions mineral chemistry, dissolved silica, pH, electrical conductivity, and the ionic forms of nitrogen, principal components analysis (PCA) treatments were used to identify and rank the main factors of variability and decipher the associated processes affecting the water chemistry. The results revealed that the water mineral concentration was a major factor of variability and it must be attributed first to lithology and second to agricultural inputs from extensive crop cultivation areas that mainly affects sulfate concentration on the eastern edge of the Pantanal. These processes influence the floodplain, where (1) the mixing of waters remains the main process, (2) the weight of the biological and redox processes increased, and (3) the chemical signature of the extensive cropping is transferred along the São Lourenço basin down to its confluence with the Cuiaba River. Optimized parameters based on projections in the main factorial score plots were used for the mapping of lithological and agricultural impacts on water chemistry.

**Keywords:** Water chemistry, PCA, Mapping, Upper Paraguay basin, Threatened wetland, Pantanal, Brazil

### **1. Introduction**

River water chemistry results from interactions between diverse hydrological, geochemical and biological processes controlled by either natural or anthropogenic determinants, namely lithology, climate, vegetation, relief, agricultural activities and domestic or industrial discharge (Stallard and Edmond, 1983; Milliman and Meade, 1983; Carpenter et al., 1998; Jarvie et al., 1998; Dupré et al., 2003; Riebe et al., 2003; Li et al., 2009; Viers et al., 2009). The relative contribution of these factors to the water chemistry of rivers shows high variability, which depends not only on the

distribution of different hydrochemical processes, the seasonal variations of precipitation and surface runoff, but also on the size of the watersheds considered (Vega et al., 1998). Studying the river chemistry allows for discovering the processes that govern the amount of dissolved species and highlighting human impact on this chemistry.

However, it is generally challenging to distinguish and quantify the weight of each process in the chemistry of rivers. A given process may influence several parameters with different intensities. Inversely, a given parameter is usually influenced by multiple processes, each with its own intensity. For example, calcium water content can be influenced by the dissolution of natural limestone, calcium carbonate inputs to correct soil pH (Waters et al., 2013), cation exchange between water and clay minerals, precipitation of carbonates due to degassing of water CO<sub>2</sub> partial pressure (Reuss and Johnson, 1985), as well as weathering of calcium silicates (Godderis et al., 2006). Therefore, the use of physical and chemical parameters to understand water character involves considering complex processes responsible for the chemistry of the hydrosystems. The analysis of these datasets with many variables generally requires multivariate statistical treatments together with geochemical and spatial analysis (Vega et al., 1998).

To trace the origin of water and the contribution of various reservoirs during floods, mixing analysis was used, first using bulk variables (chemical parameters), linear combination of these variables (Christophersen et al., 1990; Hooper et al., 1990; Ribolzi et al., 1996) and principal components for the mixing calculations (Christophersen and Hooper, 1992; Burns et al., 2001; Liu et al., 2004, Valder et al., 2012). Principal components analysis (PCA) is a classical multivariate ordination technique used to display patterns in multivariate data. It aims to graphically display the relative positions of data points in as few dimensions as possible, while retaining as much information as possible and exploring relationships between dependent variables (Syms, 2008). PCA is widely used to discriminate and rank natural or anthropogenic factors responsible for spatial or temporal variability in river hydrochemistry. Principal components furnish macro parameters that could be regarded as synthetic data conveying strong and significant information, and therefore particularly suitable for digital mapping and spatial analysis. Depending on the factor loadings, each factor can be interpreted as a hydrochemical process or combination of processes independent of the other factors but overlapping (Suk and Lee, 1999; Lawrence and Upchurch, 1982; Woocay and Walton, 2006). Each method has limitations. PCA assumes linear responses of variables, and works best over short ecological gradients. A mixing calculation requires a conservative characteristic (the absence of interaction with the environment) of the parameters across time and space of the dataset. The Upper Plata River drainage system, the second largest drainage basin in South America ( $2.8 \times 10^6$  km<sup>2</sup>), consists of two tributaries of similar importance that meet at Corrientes, Argentina: the Paraguay River, which runs in a North–South direction, and the Parana River. The major difference between these tributaries is the presence of the Pantanal floodplain located in the Paraguay headwaters. The Pantanal is considered the world's largest continental wetland ( $0.2 \times 10^6$  km<sup>2</sup>; Por, 1995), and it exerts a discernible modulating effect on the Paraguay hydrology. It is a still rather pristine wetland but increasingly threatened by large development programs. In the uplands, agroindustries and small reservoirs for hydroelectric power generation may modify discharge patterns, sediment load and water chemistry. On the other hand, plans for canalization of the Paraguay River (Hidrovia) are placing the natural flood regime of large areas inside the Pantanal at risk (Junk and Nunes de Cunha, 2005).

In a previous work, we compared the water chemistry of the 70 rivers supplying the Pantanal wetland during the wet and dry season (Rezende-Filho et al., 2012). The study highlighted a significant increase in the proportion of sulfate during the wet season that could be attributed to agricultural inputs. The time has come to establish a baseline of the water chemistry in and around the Pantanal wetland. The objective of this study, based on two datasets collected during the wet season, is to compare and identify spatial relations of the chemical diversity of the rivers in the floodplain and surrounding uplands. Together statistical and chemical analysis are used to determine whether their chemical profile reflects the mixing of the waters' diversity from the

surrounding plateaus or if it is affected by specific processes occurring in the lowlands within the Pantanal.

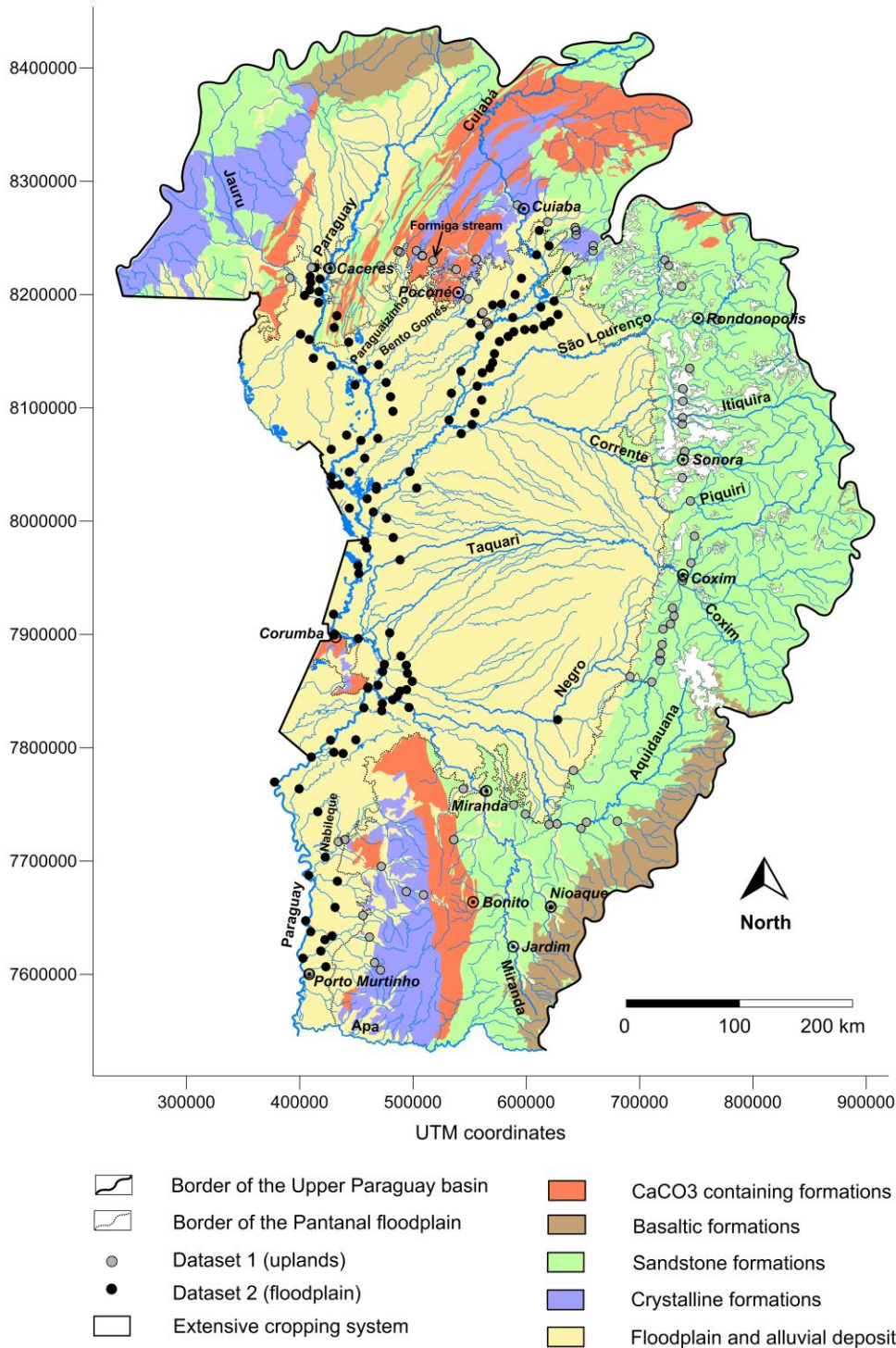


Fig. 1: Distribution of lithology, extensive crop cultivation and sampling sets in the Upper Paraguay Basin

## 2. Material and Methods

The site: The Upper Paraguay River Basin (UPRB) can be divided into two main areas: the plateaus or uplands and the Pantanal floodplain, which has been declared a Natural World Heritage site by the United Nations Educational, Scientific and Cultural Organization (UNESCO). It constitutes a

biodiversity hotspot, and also a priority region for environmental conservation (Olson and Dinerstein, 2002).

The Pantanal differs from other large continental wetlands in the world that are usually supplied by a small number of rivers. Here about 90 rivers or small watercourses flow down the floodplain along its 1300 km northern, eastern and southern border. The major tributaries are located on the left bank of the Paraguay River, namely, from north to south, the Paraguaizinho, the Bento Gomes, Cuiaba, Taquari, Negro, Miranda and Nabileque rivers. The UPRB system is largely unregulated, with the only significant dam located close to the city of Sonora on the Corrente River, a tributary of the Cuiaba River (Hamilton et al., 1997). The fluvial drainage pattern shifts from tributary to alternating distributary-tributary when the rivers enter the floodplain (Fig. 1). Because of low slopes (0.03–0.50 m/km) and as a result of torrential summer rainfall, the plain is partially covered by the flood pulse occurring from November in the northern to March in the southern part of the Pantanal, respectively (Junk and Da Cunha, 2005).

Most of the region is private land. The human population density is low in the Pantanal (<0.5 person/km<sup>2</sup>) and in most of the surrounding uplands (<4 person/km<sup>2</sup> in Mato Grosso and <7 person/km<sup>2</sup> in South Mato Grosso, IBGE 2010). In the absence of specific studies, it is usually assumed that the rivers in the UPRB are still minimally affected by human activities, except for the more populated Cuiabá River Basin (Ioris, 2013). The main impact frequently reported is an increase in sediment load due to erosion caused by recent extensive agricultural development on the upper Taquari basin (Bergier, 2013). Extensive crop cultivation is mainly developed on the plateaus of the eastern edge of the floodplain, together in an area north of the city of Pocone at the hydrological division between the Paraguaizinho and Bento Gomes basins. Primarily two kinds of crop systems are cultivated: sugar cane and a simple system of rotation of cotton, soybeans and corn. In the floodplain, the main land use activity is extensive livestock ranching.

Sampling campaigns: For this study, we used two datasets. The first dataset (dataset 1) consists of 70 samples collected during the wet season 2010 (January-February) at the headwaters of the main rivers that supply the Pantanal wetland (Rezende Filho et al., 2012). The sample set is a snapshot of the wet season chemistry in the uplands. The rivers sampled flow over various geological substrates, mainly sandstones in the east of the basin, basalts in the southeast and north, calcareous rocks in the south, north and northwest, crystalline rocks in the southwest, and interspersed throughout the sampling area. The second dataset (dataset 2, 122 samples) resulted from the aggregation of two sample collections in November 2010 (dataset 2.1) and January 2011 (dataset 2.2) along the main drainage axis of the floodplain, i.e. the Paraguay (25 samples) and Cuiaba (9 samples) rivers, and a few kilometers upstream of the confluence with their major tributaries (88 samples). The chemical composition of 8 samples collected at locations common for datasets 2.1 and 2.2 showed very similar results in terms of major ions. In addition, the water level of the Paraguay River was similar during the two sampling periods in Corumba (Ladario station, 1.29 m and 1.27 m in November and January, respectively). Therefore, these two samplings were grouped into dataset 2, which is assumed to be a snapshot of the wet season chemistry in the floodplain.

Samples were commonly collected at the center of the stream, from a bridge using a polyethylene sampler for dataset 1, and from a boat by immersing the bottle for dataset 2. Electrical conductivity (EC) and pH were measured on aliquots of 50ml. All samples were collected in duplicate and stored in the dark and at 4°C in a previously acid-washed container after 0.45µm cellulose acetate filtration.

Analytical procedure: Anions and cations were measured by ion chromatography, alkalinity by 0.1N HCl titration and silica by ICP-AES. The ionic speciation, activity, CO<sub>2</sub> partial pressure (P<sub>CO2</sub>) and the saturation with respect to carbonate minerals were calculated using AQUA database (Valles et al., 1996). The data below the detection limits (DL ~ 10<sup>-5</sup> mg l<sup>-1</sup>) for NO<sub>3</sub><sup>-</sup>, NH<sub>4</sub><sup>+</sup> and NO<sub>2</sub><sup>-</sup> were assigned to half of the detection limit value. Procedural or method blanks were below the detection limits and therefore no blank correction was applied. Results are given in supplemental Table S1 and S2.

Statistical approach: The field pH values were transformed into  $H^+$  activities to obtain a homogeneous set of parameters with  $H^+$ , EC and other water quality parameters. The 14 variables used for PCA treatments in this study are referred to as EC, H, Ca, K, Mg, Na, Cl,  $SO_4$ , Alk (carbonate alkalinity), Si,  $NO_3$ ,  $NH_4$ ,  $NO_2$ , and  $P_{CO_2}$ .

PCA was performed by diagonalization of the correlation matrix to identify, quantify and rank the factors of variability, and to explore the underlying processes affecting the water chemistry (MS excel software XLStat 2011 v2.08, Addinsoft, Paris, France). This procedure avoided the problems arising from the variable numerical ranges and units used since all variables are automatically autoscaled to the mean zero and variance unit. The PCA treatment transforms  $n$  original variables into  $n$  orthogonal principal components that are a linear combination of the original variables. Orthogonal (uncorrelated) principal components ensure the independence of the associated processes.

The treatment was first carried out on dataset 1 (PCA<sub>1</sub>, 70 samples,  $n = 13$  variables). Principal components for PCA<sub>1</sub> are referred to as  $U_1, U_2, \dots, U_{13}$ . Then, we selected 26 rivers from dataset 1 flowing on sandstone formation in the eastern Pantanal. These samples are influenced by a single lithology (sandstone) and characterized by low mineral composition, allowing for a better analysis of the non-lithological processes influencing the water chemistry. A second PCA was performed on these 26 samples including  $P_{CO_2}$  as additional variable (PCA<sub>2</sub>, 26 samples,  $n = 14$  variables). Principal components for PCA<sub>2</sub> are referred to as  $V_1, V_2, \dots, V_{14}$ .

The processing of the floodplain river chemistry (dataset 2) was performed in two ways in order to optimize the discrimination of the processes. First, the samples were plotted in the main score plots defined by PCA<sub>1</sub> in order to display the position of the floodplain samples in relation to the processes identified from the chemistry of the surrounding plateau (dataset 1). For this treatment, each variable from dataset 2 was centered on the means and divided by the standard deviations calculated from data set 1. Then the coordinates of the samples along the principal components were calculated by multiplying the standardized variables by singular values calculated from PCA<sub>1</sub>. Second, a PCA<sub>3</sub> was performed on both datasets 1 and 2 (PCA<sub>3</sub>, 192 samples, 13 variables) and the results were compared with PCA<sub>1</sub> in order to highlight the impact of the floodplain in the water chemistry. Principal components for PCA<sub>3</sub> are referred to as  $W_1, W_2, \dots, W_{13}$ .

Mapping: The distribution of the lithology and extensive cropping system was based on CRPM (2004) and CONAB (2011), respectively (Fig. 1). The mapping of the main processes identified in the study was created from the scores of the samples along the principal components using a linear variogram for the kriging (SURFER 9, Golden Software).

### 3. Results and discussion

Descriptive statistics for datasets 1 and 2 are shown in Table 1. Less mineralized waters in the basin were an Na,K/ $HCO_3$  type, whereas the most mineralized ones clearly showed a Ca,Mg/ $HCO_3$  chemical profile. The electrical conductivity of water varied from 8.3 to 515  $\mu S.cm^{-1}$ . The highest EC values were observed in the uplands for rivers flowing from the Bodoquena region, south of the Pantanal, and two of these rivers reached saturation with respect to calcite. The lowest EC values were from the Maracaju plateau, east of the floodplain. The highest variations among the variables were observed for Ca, Mg and Alk, both in the uplands (dataset 1) and in the floodplain (dataset 2).

**PCA<sub>1</sub> in the uplands (70 samples):** The correlation matrix (Table 2) shows associations between variables and some relationships can be readily inferred. The correlations with  $r$  values higher than 0.5, 0.8 and 0.9 are highlighted in the matrix (light, medium and dark grey, respectively). Several correlation coefficients are high, indicating relatively moderate complexity of the system studied, despite the geographical big size of the sampling area. High and positive correlations were observed between EC, Ca, Mg and alkalinity, indicating that waters with high mineralization are strongly influenced by calcium, magnesium and carbonate ions. A positive correlation is also observed between these variables and K, Na and Cl.  $NH_4$  showed a negative correlation with the aforementioned variables, whereas H, Si and  $SO_4$  were not correlated with any other variable.

The distribution of the inertia revealed a strongly predominant principal component  $U_1$ , which, alone, accounted for 60% of the variance, i.e. 60% of the information contained in original dataset 1. Then  $U_2$ ,  $U_3$ , and  $U_4$  explained 10%, 9%, and 6.4% of the variance, respectively. Therefore, we retained four principal components explaining 86.09% of the variance.  $U_1$ ,  $U_2$ , and  $U_3$  have eigenvalues higher than unity indicating that they contain more information than one original variable, so the decrease of dimensionality is ensured (Helena et al., 2000). Other principal components (above  $U_4$ ) accounted for a low percentage less than 5%, which makes it difficult to distinguish an associated process. Therefore these principal components were considered to comprise part of the chemical background noise of the sample set.

$U_1$  was dominated by positively correlated variables, including EC, Alk, Ca, Mg, Na, K, Cl,  $NO_2$  and  $NO_3$ , all of which were negatively correlated with H and  $NH_4$ . Electrical conductivity had the highest weight. Thus, the overall amount of dissolved ions was the main variable in the river water chemistry.  $U_2$  was mainly associated with Si, secondarily Na, and negatively correlated with  $NO_3$ ,  $NH_4$ , and H. It involved the forms of nitrogen and could be related to the biological activity and/or to the aeration of water.  $U_3$  was clearly and exclusively associated with  $SO_4$  and negatively correlated with H. It therefore was related to the mineral chemical element S and the water acidity, which depends on both the alkaline reserve and the  $CO_2$  partial pressure.  $U_4$  mainly involved the different forms of nitrogen ( $NO_3$ ,  $NO_2$ , and  $NH_4$ ) and Si.

Highlighting the water mineral concentration as a main source of variability in a dataset is a classic finding in hydrochemical studies (Mackay et al., 2011). The waters flowing over a soluble lithological substrate (limestone), or with a longer residence time, or in a more arid climate, are usually opposed to water flowing over poorly soluble rocks (sandstone, quartzites), with short residence time and in a more humid climate (Stallard and Edmond, 1983; Li et al., 2009). This aspect has been described in a previous paper based on the same dataset (Rezende-Filho et al., 2012). Waters from the eastern part of the basin flowing over sandstone formation have the lowest major ions concentration (0.05-0.3 mM). The concentration increases slightly over crystalline formation (0.3-0.8 mM), then more strongly over the basaltic basement (0.8-1.7 mM), and reaches a maximum on calcareous rocks (1.7-8.3 mM). In conclusion,  $U_1$  reflects the strong influence of the mineralization of the rivers, mainly related to the lithology.

$U_3$  is related to the sulfate content. Sulfate may have a lithological origin through dissolution of S containing evaporites or oxidation of sulfide minerals, but such minerals have not been reported in the local geology (CRPM, 2004). Other arguments support an agricultural origin of this increase in sulfate concentration. A previous study reported that higher sulfate concentration occurred only during the wet season, when surface runoff contributes in larger proportion to supply the rivers, and not during the dry season when they are mainly supplied by the baseflow (Rezende-Filho et al., 2012). Such seasonality is common in monsoonal climate regions (Li et al., 2009). In addition, the occurrence of higher sulfate concentration matched with areas of extensive corn, soybeans, sugar cane and cotton crops (Fig. 1). These crops require sulfate fertilization, and an ammonium sulfate and/or simple superphosphate that are S containing enriching agents widely recommended in soils in this region. However, it cannot be just an enrichment based on ammonium sulfate as it is an acidifying product, and here the increase in  $SO_4$  is accompanied by a slight decrease in H, i.e. an increase in the pH value. For the same reason, it cannot be attributed to anti-fungal treatment based on zinc or copper sulfates or polysulfides that acidify too. The origin of the sulfate is probably due to the application of ammonium sulfate (about  $30 \text{ kg ha}^{-1}\text{yr}^{-1}$ ) and gypsum (about  $500 \text{ kg ha}^{-1}$  every 3 years), applied together with liming, a widespread agricultural practice in the region (EMBRAPA, 2003).

Both  $U_2$  and  $U_4$  primarily involve forms of nitrogen whose contents are related to biological processes, domestic wastewater discharges, as well as agricultural inputs. The labile nature of these forms and their extreme biological reactivity quickly affects their contents in surface waters, which consequently convey fleeting information. Therefore principal components  $U_2$  and  $U_4$  are poor candidates for tracing water quality in space, and the analysis was focused on the score plots  $U_1$ - $U_3$ , which accounted for about 70% of the sample set variability (Fig. 2a).

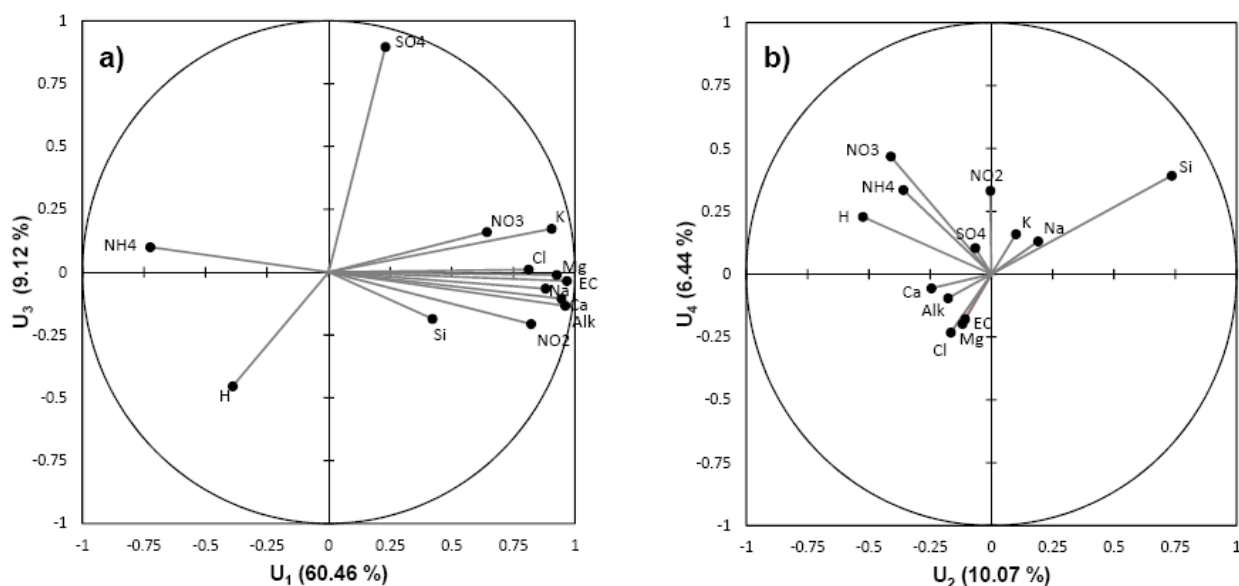


Fig. 2: Variable distribution in plots  $U_1 - U_3$  (a) and  $U_2 - U_4$  (b) for PCA<sub>1</sub>

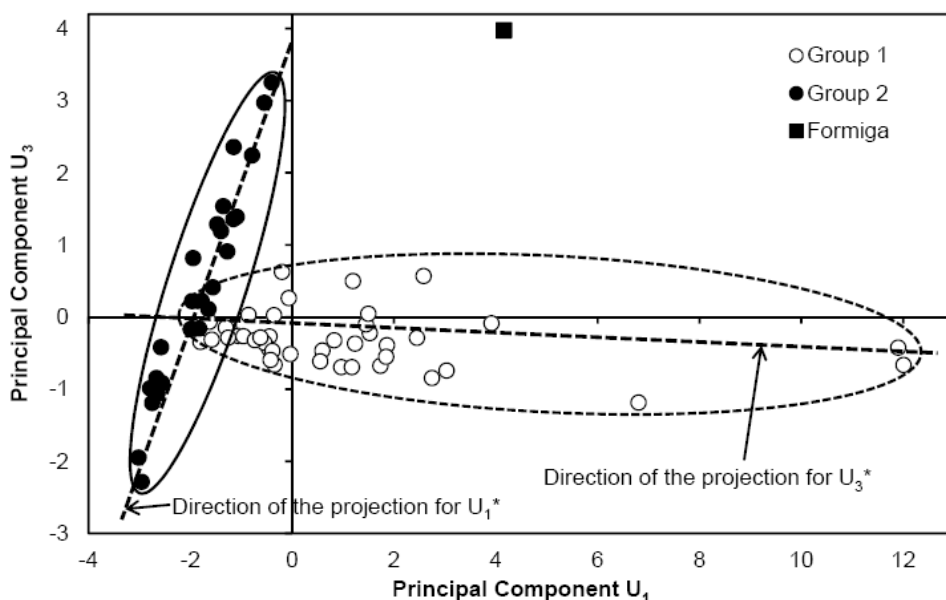


Fig. 3: Distribution of the observations from dataset 1 in scores plot  $U_1 - U_3$  for PCA<sub>1</sub> and directions of the projections for optimized  $U_1^*$  and  $U_3^*$

The distribution of dataset 1 in the  $U_1 - U_3$  score plot is presented in Fig. 3. Samples appear to be distributed within a three-component mixing diagram, but in fact, they were rather substantially distributed into two intersecting scatter plots, which visually allow for discriminating two groups. The first one, with 44 samples, was marked by an important change in the sample mineral concentration along  $U_1$ , although without significant change, just a slight decrease, along  $U_3$ . Therefore, this group showed a wide range of mineral concentration, which is related to the lithology. The second group of 26 samples was characterized by low mineral concentration but a sharp increase along  $U_3$ , i.e. an increase in  $SO_4$  and pH values attributed to agricultural inputs. Samples from group 1 are located in crystalline, basalt, and calcareous formations, whereas samples from group 2 are east of the Pantanal wetland and on sandstone formations providing waters with very low mineral concentration. The Formiga stream originates from calcareous rocks and was strongly marked by both a higher mineral concentration and the high  $SO_4$  value. Therefore it differed from groups 1 and 2 in Fig. 3.



For the second group of samples, part of the mineral concentration is related to the gain of sulfate provoking a slight inclination of the scatter plot along  $U_1$ . Consequently, the  $PCA_1$  treatment mixed up both sources of variability.  $U_1$  represents the mineralization induced by the regional lithology, but it also conveys the increase in the water mineral concentration related to anthropogenic sulfate inputs. However, it is possible to assess the non-anthropogenic component of the mineral concentration by projecting the plot along  $U_1$  and parallel to the direction of the second scatter plot (group 2). This adjusted parameter  $U_1^*$  reflects the water mineral concentration not related to sulfate agricultural inputs, i.e., mainly a lithological mineral concentration. Similarly, a projection of the plot along  $U_3$  and parallel to scatter plot of group 1 provides an adjusted parameter  $U_3^*$ , which mainly reflects the effect of agricultural inputs on the water chemistry. These adjusted parameters  $U_1^*$  and  $U_3^*$  will be used in the latter paragraph for mapping.

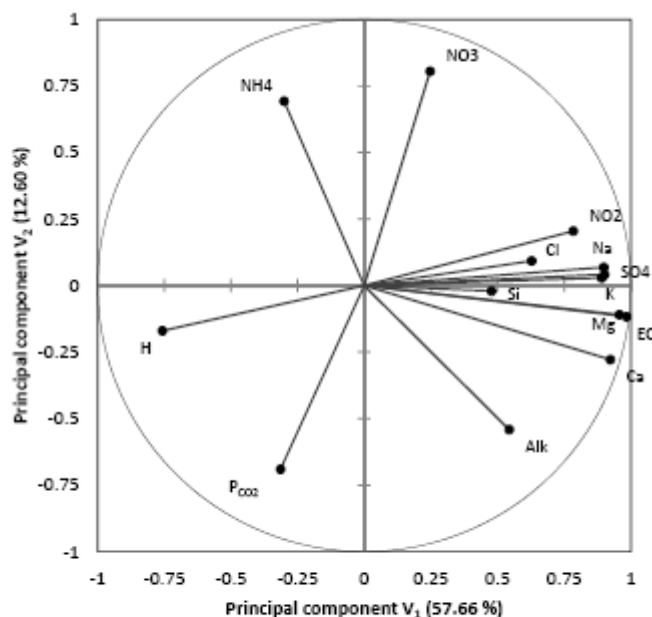


Fig. 4: Distribution of the variables in plot  $V_1$ - $V_2$  for  $PCA_2$  (26 obs.)

**PCA<sub>2</sub> on upland sandstone lithology (group 2 - 26 samples):** In order to better understand the chemical processes occurring in the area strongly influenced by the agricultural inputs, a  $PCA_2$  was carried out on group 2 including calculated  $P_{CO_2}$  as an additional variable. The pH values of the dataset are field measurement values. Therefore, assuming that the alkalinity does not change from the collection to the analysis, the calculated  $P_{CO_2}$  corresponds to field conditions. The first principal component  $V_1$  captured 57.7% of variation in the dataset chemistry (Fig. 4).  $V_1$  was strongly associated with EC, Alk, Ca, Mg, and also  $SO_4$ , and negatively correlated with H. The position of the variable  $SO_4$ , close to EC in the factorial plan  $V_1$ - $V_2$ , shows that sulfate concentrations contributed significantly to the mineral concentration of the waters in this group. This aspect confirms that it was necessary to adjust  $U_1$  into  $U_1^*$  in the previous  $PCA_1$ , in order to erase the human contribution generated by agricultural inputs to assess the lithological mineral concentration.  $V_2$ , which accounted for 12.6% of the variance, was associated with  $NO_3$  and  $NH_4$  and negatively correlated with  $P_{CO_2}$  and alkalinity. This finding could correspond to an opposition between oxic water with low  $CO_2$  where  $NO_3$  persists, and anoxic waters with higher  $CO_2$  where denitrification occurs. The location of  $NH_4$  in the plan is not fully in agreement with this interpretation, but  $NH_4$  contents also depend on ammonium sulfate inputs that vary from place to place.

**Floodplain samples (dataset 2) plotted in  $PCA_1$ :** The waters from the floodplain were ordered into six groups according to their origin, i.e., water from the Paraguay and from its tributaries of

right or left bank and water from the Cuiaba and from its tributaries of the right or left banks. Fig. 5 displays the mean values and standard deviation for each group and for dataset 1 collected on the uplands.

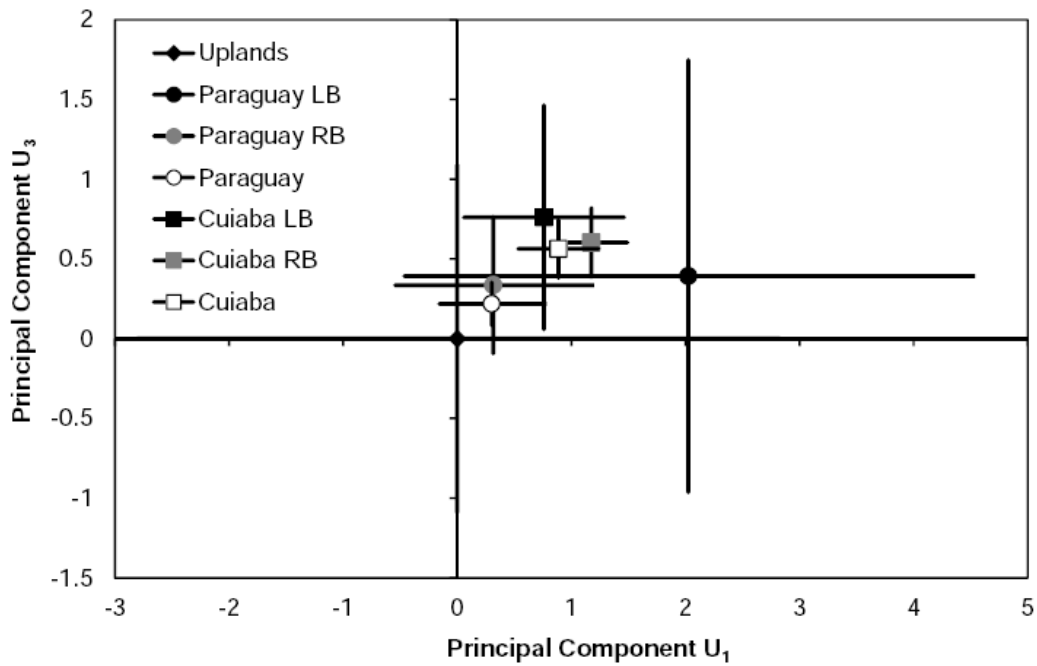


Fig. 5: Mean value and standard deviation for data set 1 and 2 in plot  $U_1$ - $U_3$  for  $PCA_1$   
 LB: Tributaries on the left bank, RB: Tributaries on the right bank

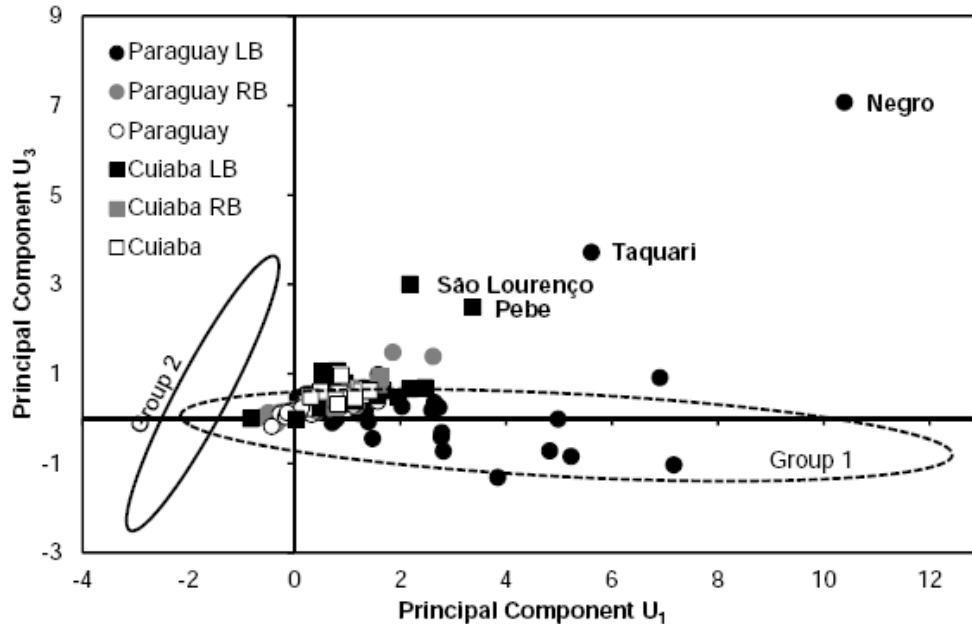


Fig. 6: Distribution of observations from data set 2 in plot  $U_1$ - $U_3$  for  $PCA_1$   
 Envelopes for groups 1 and 2 refer to Fig.3.  
 LB: Tributaries on the left bank, RB: Tributaries on the right bank

The mean values of the six groups were located in the top-right quadrant on score plot  $U_1$ - $U_3$ , i.e. with positive scores. The standard deviations were high for dataset 1 and for the tributaries of the right bank of the Paraguay River; i.e. for the waters originating from the uplands and/or with a

smaller contributive area. Then the standard deviation decreased in the floodplain with increasing watershed area. This result is standard in hydrosystems but particularly clear in our data, as the successive confluences increase the volume of the hydrosystem, leading to mixed waters with more stable chemical characteristics and closer to the mean value. These findings confirm that it was relevant to scale the variables from the mean values and standard deviations calculated from dataset 1.

Fig. 6 shows samples from dataset 2 plotted in score plot  $U_1$ - $U_3$ . Most of the samples were located within the envelope delimited by the samples from dataset 1, confirming the relevance of the treatment. Most of the rivers supplying the Cuiaba and Paraguay Rivers were located close to the samples of group 1, suggesting that the influence of the agricultural input is less in the floodplain. Mainly four samples differed from the scatter plot: two were mineralized waters collected at the confluence of the Negro and Taquari Rivers with the Paraguay. These waters had slightly higher  $SO_4$  but together with high  $NO_3$  and  $NH_4$ , which typically characterizes local redox processes that could be related to the presence of some animal carcasses observed along the stream. The sample collected about 30 km upstream of the confluence of the Negro River did not show any  $SO_4$  nor  $NO_3$  increase. Therefore the chemical characteristic observed close to the confluence are more likely temporary than permanent pollution. The other two samples were moderately mineralized waters from the São Lourenço River and its distributary (the Pebe stream) just upstream from their junction with the Cuiaba River. The main change in the chemical composition was an increase in  $SO_4$  of about 0.05 to 0.1 mM; i.e. in similar proportions to what was observed upriver on the plateau. Therefore, we postulate that the chemical changes provoked by the agricultural inputs are reflected in the floodplain, down to the confluence with the Cuiaba River.

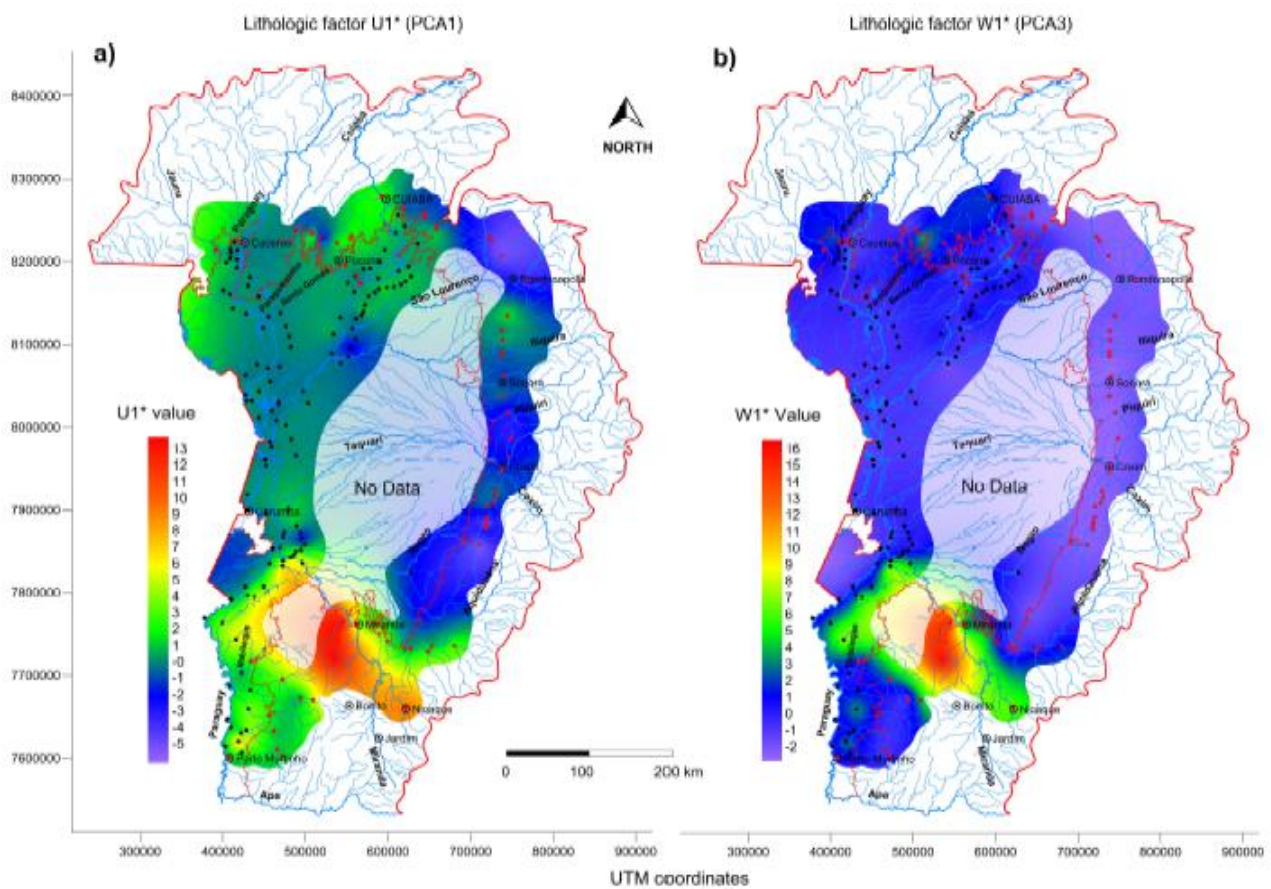


Fig. 7

Fig. 7: Distribution of the lithological factor based on (a)  $PCA_1$  and (b)  $PCA_3$  treatments.

**$PCA_3$  carried out on datasets 1 and 2 (192 samples):**  $PCA_3$  highlighted principal components very similar to those revealed by  $PCA_1$ , indicating that both  $PCA_1$  and  $PCA_3$  detected the same

processes. However, the ranking of the principal components changed when compared to PCA<sub>1</sub>. U<sub>1</sub> and U<sub>3</sub>, which accounted for 70% of the inertia, were roughly similar to W<sub>1</sub> and W<sub>4</sub>, associated with the same variables and in similar proportion, but with a net decrease to 50% of the inertia in PCA<sub>3</sub>. In parallel, a strengthening of biological processes was observed shifting from 16% (U<sub>2</sub> and U<sub>4</sub> in PCA<sub>1</sub>) to 21% (W<sub>2</sub> and W<sub>3</sub> in PCA<sub>3</sub>), indicating that several samples in the floodplain were significantly affected by the redox conditions.

The sample distribution in score plot W<sub>1</sub>-W<sub>4</sub> for PCA<sub>3</sub> were very similar to those in score plot U<sub>1</sub>-U<sub>3</sub> for PCA<sub>1</sub>, highlighting two groups of observations from the uplands, demonstrating that the principal components convey roughly the same information. Consequently and similar to what was determined following the study of PCA<sub>1</sub>, it was possible to define two factors optimizing the information conveyed in score plot W<sub>1</sub>-W<sub>4</sub>. The first one is a lithological factor W<sub>1</sub><sup>\*</sup>, which corresponds to a projection along W<sub>1</sub> parallel to the scatter plot of group 2. The second one, W<sub>4</sub><sup>\*</sup>, mainly influenced by sulfate concentration is a factor of agricultural pollution, and corresponds to the projection along W<sub>4</sub> parallel to the scatter plot of group 1. These adjusted factors W<sub>1</sub><sup>\*</sup> and W<sub>4</sub><sup>\*</sup> were used for the mapping.

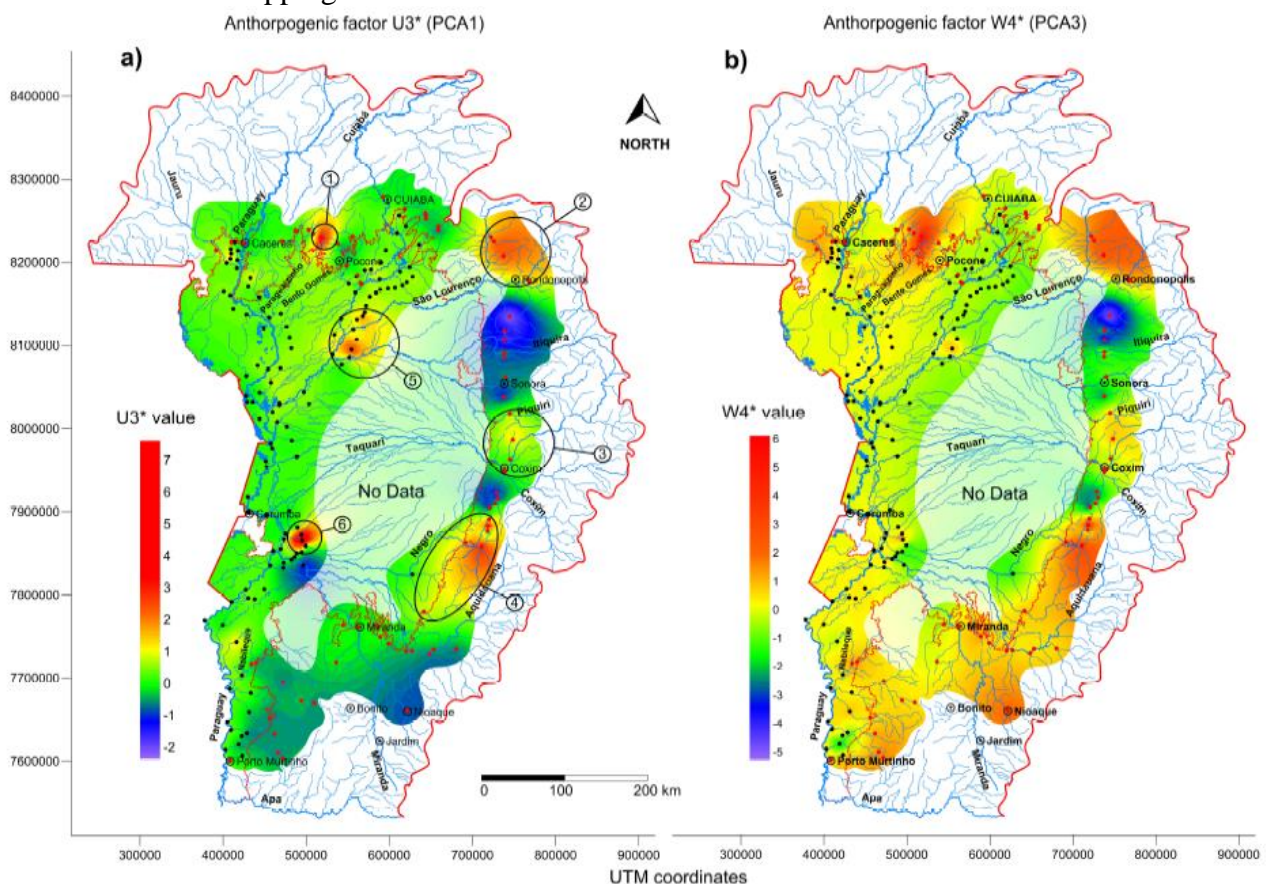


Fig. 8

Fig. 8: Distribution of the anthropogenic factor based on (a) PCA<sub>1</sub> and (b) PCA<sub>3</sub> treatments.

**Mapping:** The distribution of both the lithological factor (U<sub>1</sub><sup>\*</sup> and W<sub>1</sub><sup>\*</sup>) and the influence of extensive agriculture, referred to henceforth as an anthropogenic factor (U<sub>3</sub><sup>\*</sup> and W<sub>4</sub><sup>\*</sup>) are drawn in the upper Paraguay basin (Figures 7 and 8). In regards to the same processes identified in both cases, we should expect rather similar maps in Figs. 7a and 7b, and in Figs 8a and 8b. However, after processing of all the samples (W<sub>1</sub><sup>\*</sup> and W<sub>4</sub><sup>\*</sup>) the results appear less contrasted for the distribution of both the lithological (Fig. 7b) and anthropogenic (Fig. 8b) factors. Because of a higher number of samples; i.e. 192 compared to 70, the information sought (lithological and anthropogenic factors) is diluted in the greater total information. Thus, the PCA<sub>1</sub> treatment conducted only on dataset 1, optimized by projections within the score plot U<sub>1</sub>-U<sub>3</sub>, and then followed by the injection of the samples of the floodplain showed to be the most effective in

discriminating these two factors for mapping. The data processing (Fig. 7a) clearly highlighted the influence of calcareous rocks in the Bodoquena region, south of the Pantanal but also, albeit less pronounced, in the upper Cuiaba and lower Jauru basins. This highlighted the influence of basalt in the southeastern Aquidauana and upper Miranda basins. The eastern edge of the Pantanal, which is characterized by water flowing over sandstone, appeared relatively uniform. Finally, this treatment showed that the chemistry of the Paraguay River is influenced downstream of its confluence with the Miranda, by the mineralized water from the Bodoquena uplands. Although the evaporative concentration is frequently a major factor influencing large wetlands (Mackay et al., 2011) and more specifically in a large sub-region of the Pantanal (Furian et al., 2013), it has had little effect on the studied hydrological network.

In the uplands, the anthropogenic factor is divided into four spots (Fig. 8a), between Cáceres and Poconé on the Formiga stream (1 on Fig. 8a), north of the city of Rondonópolis (2), between Sonora and Coxim (3), and on the upper Negro basin (4). The spot identified in the floodplain at the confluence between the Cuiaba and São Lourenço must be attributed to a transfer of pollution throughout the São Lourenço basin (5). Finally, the spot located at the confluence of the Negro and Taquari with Paraguay (6) provided a mixture of information conveyed by factor  $U_3^*$ , which is most likely a local and fleeting pollution phenomenon.

Sulfate is known to leach into inland aquatic ecosystems. The rates of accumulation of reduced sulfur compounds in wetlands can be quite rapid, particularly in the case of distributary flooding in the Pantanal. Even short-term exposure to elevated levels of sulfate can lead to the accumulation of sufficient reduced sulfur compounds in sediment to be of concern if they are disturbed, and it is increasingly seen as an issue in wetland management (Lamers et al., 1998; Lamers et al., 2001). Sulfate addition affects the way that carbon is processed in wetlands (Reddy and DeLaune, 2008; Baldwin and Mitchell, 2012), and changing such a fundamental process could significantly impact the biogeochemical functioning of wetlands.

#### **4. Conclusion**

The variability in river water chemistry in the upper Paraguay basin is largely unknown in this poorly studied region, mainly because of the sparse population, long distances and lack of roads for access to sampling points. This study provides a baseline of water chemistry from which to monitor future changes in and around the Pantanal wetland. The results confirm the geochemical zonation of major ions mainly controlled by the lithology of uplands. The mixing of water remains the main process in the Pantanal floodplain together with a strengthening of the redox processes. This study highlights an increase in sulfate content that mainly affects areas developed on sandstone formations, and some calcareous areas north of the Pantanal. The increase in sulfate contents (by a factor of about 10) is likely from agricultural origin and reflected in the floodplain along the São Lourenço basin down to its confluence with the Cuiaba. With these conventional human activities, the implication of increasing sulfates remains unknown, but can potentially be profound, and, therefore, must be monitored in the future.

#### **5. Acknowledgements**

This research was supported by grants from the Coordination of Improvement of Higher Education Personnel (CAPES), the Consulate of France in São Paulo and São Paulo University to L. Barbiero, and by Centro Nacional de Desenvolvimento Científico e Tecnológico (CNPq) to A.T. Rezende-Filho (248550/2012-8). It was funded by the Sao Paulo Research Foundation (FAPESP, 2011/12770-0) and CNPq (405898/2012-6). We thank A. Ayres Montebelo for performing chemical analysis. We are very grateful to the Brazilian Navy (6<sup>th</sup> Naval District of Ladario) for the logistical support along the Paraguay and Cuiaba Rivers. Jim Hesson of AcademicEnglishSolutions.com revised the English.

#### **6. References**

- Baldwin, D.S., and A. Mitchell. 2012. Impact of sulfate pollution on anaerobic biogeochemical cycles in wetland sediment, *Water Res.*, 46:965–974, DOI:10.1016/j.watres.2011.11.065
- Bergier, I. 2013. Effects of highland land-use over lowlands of the Brazilian Pantanal. *Science of The Total Environment* 463–464:1060–1066. DOI:10.1016/j.scitotenv.2013.06.036
- Burns, D.A., J.J. McDonnell, R.P. Hooper, N.E. Peters, J.E. Freer, C. Kendall, and K. Beven. 2001. Quantifying contributions to storm runoff through end-member mixing analysis and hydrologic measurements at the Panola Mountain Research Watershed (Georgia, USA). *Hydrological Processes* 15:1903-1924. DOI:10.1002/hyp.246
- Carpenter, S.R., N.F. Caraco, D.L. Correll, R.W. Howarth, A.N. Sharpley, and V.H. Smith. 1998. Non-point pollution of surface waters with phosphorus and nitrogen. *Ecol. Appl.* 8:559–568. DOI:10.1890/1051-0761(1998)008[0559:NPOSWW]2.0.CO;2
- Christophersen, N., C. Neal, R.P. Hooper, R.D. Vogt, and S. Andersen. 1990. Modeling streamwater chemistry as a mixture of soilwater end-members - A step towards 2<sup>nd</sup> generation acidification models. *Journal of Hydrology* 116:307-320. DOI:10.1016/0022-1694(90)90130-P
- Christophersen, N., R.P. Hooper. 1992. Multivariate-analysis of stream water chemical data - The use of principal component analysis for the end-member mixing problem. *Water Resources Research* 28:99-107. DOI:10.1029/91WR02518
- CONAB, 2011. Brazilian crop assessment, grain, crop 2010/2011, <http://geoweb.conab.gov.br/conab/>. National Company of Food Supply (CONAB), Brasilia.
- CPRM, 2004. Geological map of Brazil 1/1,000,000. Geographic information system – GIS. Serviço Geológico do Brasil – CPRM, 41 CD-ROM (ISBN 85-7499-009-4), Brasilia.
- Dupre, B., C. Dessert, P. Oliva, Y. Godderis, J. Viers, L. François, R. Millot, and J. Gaillardet. 2003. Rivers, chemical weathering and Earth's climate. *Comptes Rendus Geosci.* 335:1141–1160. DOI:10.1016/j.crte.2003.09.015.
- EMBRAPA. 2003. Cultura do Algodão no Cerrado. Electronic version. <http://sistemasdeproducao.cnptia.embrapa.br/FontesHTML/Algodao/AlgodaoCerrado/adubacao.htm>
- Furian, S., E.C.R. Martins, T.M. Parizotto, A.T. Rezende-Filho, R.L. Victoria, and L. Barbiero. 2013. Chemical diversity and spatial variability in myriad lakes in Nhecolândia in the Pantanal wetlands of Brazil. *Limnol. Oceanogr.* 58:2249–2261. DOI:10.4319/lo.2013.58.6.2249
- Godderis, Y., L. François, A. Probst, J. Schott, D. Moncoulon, D., Labat, and D. Virille. 2006. Modelling weathering processes at the catchment scale: The WITCH numerical model. *Geochimica et Cosmochimica Acta* 70:1128-1147. DOI:10.1016/j.gca.2005.11.018
- Hamilton, S.K., S.J. Sippel, D.F. Calheiros, and J.M. Melack. 1997. An anoxic event and other biogeochemical effects of the Pantanal wetland on the Paraguay River, *Limnology and Oceanography* 42:257–272.
- Helena, B., R. Pardo, M. Vega, E. Barrado, J.M. Fernandez, and L. Fernandez. 2000. Temporal evolution of groundwater composition in an alluvial aquifer (Pisuerga river, Spain) by principal component analysis. *Water Res.* 34:807-816. DOI:10.1016/S0043-1354(99)00225-0
- Hooper, R.P., N. Christophersen, and N.E. Peters. 1990. Modeling streamwater chemistry as a mixture of soilwater end-members – An application to the Panola mountain catchment, Georgia, USA. *Journal of Hydrology* 116:321-343. DOI:10.1016/0022-1694(90)90131-G
- IBGE, 2010. <http://censo2010.ibge.gov.br/>
- Ioris, A.A.R., 2013. Rethinking Brazil's Pantanal wetland: beyond narrow development and conservation debates. *Journal of Environment & Development* 22:239-260. DOI:10.1177/1070496513493276
- Jarvie, H.P., B.A. Whitton, and C. Neal. 1998. Nitrogen and phosphorus in east-coast British rivers: speciation, sources and biological significance. *Sci. Total Environ.* 210/211:79–109. DOI:10.1016/S0048-9697(98)00109-0.
- Junk, W.J., and C.N. da Cunha. 2005. Pantanal: a large South American wetland at a crossroads. *Ecological Engineering* 24:391-401. DOI:10.1016/j.ecoleng.2004.11.012

- Lamers, L.P.M., H.B.M. Tomassen, and J.G.M. Roelofs. 1998. Sulfate induced eutrophication and phytotoxicity in freshwater wetlands. *Environmental Science and Technology* 32:199-205. DOI:10.1021/es970362f
- Lamers, L.P., M.G.E. Ten Dolle, S.T.G. Van Denberg, S.P.J. Van Delft, and J.G.M. Roelofs. 2001. Differential responses of freshwater wetland soils to sulphate pollution. *Biogeochemistry* 55:87-102. DOI:10.1023/A:1010629319168
- Lawrence, F.W., and S.B. Upchurch. 1982. Identification of recharge areas using geochemical factor analysis. *Ground Water* 20:680-687.
- Li, S., S. Gu, X. Tan, and Q. Zhang. 2009. Water quality in the upper Han River basin, China: the impacts of land use/land cover in riparian buffer zone. *J. Hazard. Mater.* 165:317-324. DOI:10.1016/j.jhazmat.2008.09.123
- Liu, F., M. Williams, and N. Caine. 2004. Source waters and flowpaths in a seasonally snow-covered catchment, Colorado Front Range, USA. *Water Resources Research* 40:W09401. DOI:10.1029/2004WR003076
- Mackay, A.W., T. Davidson, P. Wolski, R. Mazebedi, W.R.L Masamba, P. Huntsman-Mapila, and M. Todd. 2011. Spatial and Seasonal Variability in Surface Water Chemistry in the Okavango Delta, Botswana: A Multivariate Approach. *Wetlands* 31:815-829. DOI:10.1007/s13157-011-0196-1.
- Milliman, J.D., and R.H. Meade. 1983. World-wide delivery of river sediments to the oceans. *The Journal of Geology* 91:1-21 1. DOI:10.1086/628741
- Olson, D. M., and E. Dinerstein. 2002. The Global 200: Priority ecoregions for global conservation. *Annals of the Missouri Botanical Garden*, 89:199-224.
- Por, F.D. 1995. *The Pantanal of Mato Grosso (Brazil): World's Largest Wetlands*. Monographiae Biologicae, Springer.
- Reddy, K.R., and R.D. DeLaune. 2008. *Biogeochemistry of wetlands: Science and applications*. CRC Press Inc., Boca Raton, USA.
- Reuss, J.O., and D.W. Johnson. 1985. Effect of soil processes on the acidification of water by acid deposition. *J. Environ. Qual.* 14:26-31. DOI:10.2134/jeq1985.00472425001400010005x
- Rezende-Filho, A.T., Furian, S., Victoria, R.L., Mascré, C., Valles, V., Barbiero, L., 2012. Hydrochemical variability at the Upper Paraguay Basin and Pantanal wetland. *Hydrology and Earth System Science* 16:2723-2737. DOI:10.5194/hess-16-2723-2012
- Ribolzi, O., V. Valles, and T. Bariac. 1996. Comparison of hydrograph deconvolutions using residual alkalinity. *Water Res. Resource* 32:1051–1059. DOI:10.1029/95WR02967
- Riebe, C.S., J.W. Kirchner, and R.C. Finkel. 2003. Long-term rates of chemical weathering and physical erosion from cosmogenic nuclides and geochemical mass balance. *Geochim. Cosmochim. Acta* 67:4411–4427.
- Stallard, R.F., and J.M. Edmond. 1983. Geochemistry of the Amazon: 2. the influence of geology and weathering environment on the dissolved load. *J. Geophys. Res.* 88:9671–9688. DOI: 10.1029/JC088iC14p09671.
- Suk, H., and K.K. Lee. 1999. Characterization of a ground water hydrochemical system through multivariate analysis: Clustering into ground water zones. *Ground Water* 37:358-366.
- Syms C., 2008. Reference Module in Earth Systems and Environmental Sciences. *Encyclopedia of Ecology* 2940-2949.
- Valder, J.F., A.J. Long, A.D. Davis, and S.J. Kenner. 2012. Multivariate statistical approach to estimate mixing proportions for unknown end members. *Journal of Hydrology* 460-461:65-76. DOI:10.1016/j.jhydrol.2012.06.037
- Valles, V., O. Ribolzi, A.M. de Cockborne, and M. Cornieles. 1996. Presentation de AQUA, logiciel de géochimie appliqué aux problèmes environnementaux. GRESSAP, 10 September 1996. ORSTOM, Montpellier.
- Vega, M., R. Pardo, E. Barrado, and L. Deban. 1998. Assessment of seasonal and polluting effects on the quality of river water by exploratory data analysis. *Water Res.* 32:3581-3592. DOI:10.1016/S0043-1354(98)00138-9.

- Viers, J., B. Dupré, and J. Gaillardet. 2009. Chemical composition of suspended sediments in World Rivers: New insights from a new database. *The Science of the Total Environment* 407:853-868. DOI:10.1016/j.scitotenv.2008.09.053
- Waters, M.N., J.M. Smoak, and C.J. Saunders. 2013. Historic primary producer communities linked to water quality and hydrologic changes in the northern Everglades. *J. Paleolimnol.* 49:67–81. DOI:10.1007/s10933-011-9569-y
- Woocay, A., and J. Walton. 2006. Multivariate Analyses of Water Chemistry: Surface and Ground Water Interactions. *Ground Water* 46:437-449. DOI:10.1111/j.1745-6584.2007.00404.x

Fig. 1: Distribution of lithology, extensive crop cultivation and sample sets in the Upper Paraguay Basin

Fig. 2: Variable distribution in plots  $U_1-U_3$  (a) and  $U_2-U_4$  (b) for  $PCA_1$

Fig. 3: Distribution of the observations from dataset 1 in scores plot  $U_1-U_3$  for  $PCA_1$ , and directions of the projections for optimized  $U_1^*$  and  $U_3^*$

Fig. 4: Distribution of the variables in plot  $V_1-V_2$  for  $PCA_2$  (26 obs.)

Fig. 5: Mean value and standard deviation for dataset 1 and 2 in score plot  $U_1-U_3$  for  $PCA_1$ . LB: Tributaries on the left bank, RB: Tributaries on the right bank

Fig. 6: Distribution of observations from dataset 2 in plot  $U_1-U_3$  for  $PCA_1$ . Envelopes for groups 1 and 2 refer to Fig.3. LB: Tributaries on the left bank, RB: Tributaries on the right bank

Fig. 7: Distribution of the lithological factor based on (a)  $PCA_1$  and (b)  $PCA_3$  treatments.

Fig. 8: Distribution of the anthropogenic factor based on (a)  $PCA_1$  and (b)  $PCA_3$  treatments.

Table 1: Table 1: Descriptive statistics for dataset 1 (70 samples) and dataset 2 (122 samples).

Table 2: Correlation matrix of the 13 physico-chemical parameters on dataset 1 (70 samples)

Table S1 : Coordinates, field measurements and chemical composition of sample set 1 (Uplands, 70 samples)

Table S2 : Coordinates, field measurements and chemical composition of sample set 2 (Uplands, 122 samples)



Table 1: Descriptive statistics for dataset 1 (70 samples) and dataset 2 (122 samples).

Physico-chemical Parameter	Variable name	Data Below DL	Unit	Dataset 1				Dataset 2			
				Min.	Max.	Mean value	Standard deviation	Min.	Max.	Mean value	Standard deviation
Electrical conductivity	EC	0	$\mu\text{S cm}^{-1}$	8.3	515	85.3	90.2	18	313	67	40.4
pH (converted into $\text{H}^+$ )	H	0	mM	$5.8 \times 10^{-9}$	$5.9 \times 10^{-6}$	$5.3 \times 10^{-7}$	$1.1 \times 10^{-6}$	$1.1 \times 10^{-8}$	$8.9 \times 10^{-7}$	$1.6 \times 10^{-7}$	$1.6 \times 10^{-7}$
Calcium	Ca	0	mM	$2 \times 10^{-3}$	1.65	0.17	0.292	$9 \times 10^{-3}$	0.86	0.12	0.120
Potassium	K	0	mM	$6 \times 10^{-3}$	0.07	0.02	0.013	$2.2 \times 10^{-2}$	0.128	0.05	0.021
Magnesium	Mg	0	mM	$2 \times 10^{-4}$	1.04	0.11	0.162	$1.4 \times 10^{-2}$	0.544	0.10	0.073
Sodium	Na	0	mM	$1.3 \times 10^{-2}$	0.28	0.06	0.053	$6 \times 10^{-3}$	0.15	0.05	0.025
Chloride	Cl	0	mM	$2 \times 10^{-3}$	0.18	0.03	0.029	$5 \times 10^{-3}$	0.22	0.04	0.028
Sulfate	SO4	0	mM	$2 \times 10^{-3}$	0.16	0.02	0.030	$2 \times 10^{-3}$	0.102	0.02	0.013
Carbonate alkalinity	Alk	0	mM	$9 \times 10^{-3}$	5.21	0.58	0.889	$6.2 \times 10^{-2}$	2.85	0.47	0.392
Silica	Si	0	mM	$4.8 \times 10^{-2}$	0.39	0.12	0.066	$1.9 \times 10^{-2}$	0.22	0.13	0.028
Nitrate	NO3	1	mM	$8 \times 10^{-5}$	0.05	$6 \times 10^{-3}$	0.007	$1.6 \times 10^{-4}$	0.28	$1.3 \times 10^{-2}$	0.028
Ammonium	NH4	4	mM	$2 \times 10^{-5}$	0.03	$1.6 \times 10^{-2}$	0.010	$1.9 \times 10^{-5}$	0.02	$2 \times 10^{-3}$	$3 \times 10^{-3}$
Nitrite	NO2	3	mM	$1.6 \times 10^{-4}$	$1.4 \times 10^{-2}$	$10^{-3}$	0.002	$1.3 \times 10^{-4}$	$3.3 \times 10^{-2}$	$1.4 \times 10^{-3}$	$4 \times 10^{-3}$

Table 2: Correlation matrix of the 13 physico-chemical parameters on dataset 1 (70 samples)

	EC	H	Ca	K	Mg	Na	Cl	SO <sub>4</sub>	Alk	Si	NO <sub>3</sub>	NH <sub>4</sub>	NO <sub>2</sub>
EC	1.000												
H	-0.333	1.000											
Ca	0.961	-0.244	1.000										
K	0.821	-0.395	0.793	1.000									
Mg	0.946	-0.293	0.901	0.807	1.000								
Na	0.827	-0.335	0.765	0.806	0.749	1.000							
Cl	0.832	-0.284	0.815	0.630	0.766	0.640	1.000						
SO <sub>4</sub>	0.187	-0.250	0.118	0.384	0.228	0.159	0.186	1.000					
Alk	0.977	-0.260	0.987	0.813	0.951	0.799	0.798	0.099	1.000				
Si	0.280	-0.303	0.223	0.457	0.249	0.556	0.220	-0.025	0.266	1.000			
NO <sub>3</sub>	0.576	-0.141	0.667	0.591	0.491	0.542	0.477	0.257	0.611	0.083	1.000		
NH <sub>4</sub>	-0.717	0.376	-0.594	-0.648	-0.673	-0.676	-0.515	-0.080	-0.648	-0.416	-0.184	1.000	
NO <sub>2</sub>	0.710	-0.205	0.783	0.772	0.712	0.692	0.556	0.038	0.788	0.456	0.604	-0.505	1.000